

# Tunable Heterogeneous Catalysis: N-Heterocyclic Carbenes as Ligands for Supported Heterogeneous Ru/K-Al<sub>2</sub>O<sub>3</sub> Catalysts To Tune Reactivity and Selectivity

Johannes B. Ernst,<sup>†</sup> Satoshi Muratsugu,<sup>\*,‡</sup> Fei Wang,<sup>‡</sup> Mizuki Tada,<sup>‡,§,||</sup> and Frank Glorius<sup>\*,†</sup>

<sup>†</sup>Organisch-Chemisches Institut, Westfälische Wilhelms-Universität Münster, Corrensstrasse 40, 48149 Münster, Germany

<sup>‡</sup>Department of Chemistry, Graduate School of Science, <sup>§</sup>Research Center for Materials Science (RCMS), and <sup>||</sup>Integrated Research Consortium on Chemical Sciences (IRCCS), Nagoya University, Furo-cho, Chikusa, Nagoya, Aichi 464-8602, Japan

**S** Supporting Information

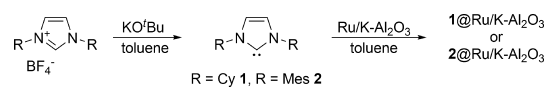
**ABSTRACT:** Here we report, for the first time, an extensive characterization of an N-heterocyclic carbene (NHC)-modified supported heterogeneous catalyst. The existence of the metal-carbene bond could be proven by <sup>13</sup>C-SS-NMR experiments. Furthermore, it could be shown that the modification with NHCs does not structurally change the catalyst itself. The effect of the nature and the loading of the NHC on the activity and selectivity of the heterogeneous catalyst is presented by a hydrogenation study, finally leading to an NHC-enabled tunable heterogeneous catalyst for chemoselective hydrogenation.

In coordination chemistry and homogeneous catalysis, N-heterocyclic carbenes (NHCs) are well-known and widely applied ligands. Due to their electron-rich nature, they act as strong  $\sigma$ -donor and weak  $\pi$ -acceptor ligands and can form strong bonds to metals.<sup>1</sup> This significantly influences the reactivity and selectivity of metal complexes and leads to widespread application in the fields of cross-coupling<sup>2</sup> and metathesis.<sup>3</sup> Their application for the stabilization of nanoparticles (NPs) and surfaces has increased considerably over the past decade.<sup>4,5</sup> Starting with Au-NPs, the groups of Chechik<sup>6</sup> and Tilley<sup>7</sup> could employ NHCs for the stabilization of NPs. The groups of Chaudret,<sup>8</sup> Ravoo, and Glorius<sup>9</sup> were able to further apply NHCs in the stabilization of catalytically active Ru, Pt, and Pd-NPs. Very recently, Johnson et al. could use NHC-stabilized Au-NPs for biological applications.<sup>10</sup> However, the application of NHCs to modify metal-oxide or carbon-supported heterogeneous catalysts is, to the best of our knowledge, limited to one seminal paper by Glorius et al.,<sup>11</sup> where enantioenriched NHCs are applied as ligands in the asymmetric  $\alpha$ -arylation of ketones using Pd/Fe<sub>3</sub>O<sub>4</sub> as catalyst.

In general, supported heterogeneous catalysts are, without doubt, the most important catalysts in industrial chemistry.<sup>12</sup> Due to their robustness, high recyclability, and ease of handling, they have significant advantages over homogeneous catalyst systems. Therefore, it is striking that there is only one example of merging the advantages of NHCs as well-known ligands in homogeneous catalysis with the advantages and industrial importance of supported heterogeneous catalysts.<sup>11</sup>

Based on the fact that there is, in contrast to unsupported NPs,<sup>6–10</sup> no understanding of the binding mode of NHCs to

## Scheme 1. Schematic Approach for the Modification of Ru/K-Al<sub>2</sub>O<sub>3</sub> with NHCs



supported heterogeneous catalysts, we wanted to investigate the direct modification of Ru-NPs supported on potassium-doped alumina (Ru/K-Al<sub>2</sub>O<sub>3</sub>)<sup>13</sup> with NHCs. We chose Ru/K-Al<sub>2</sub>O<sub>3</sub> as its activity in hydrogenation reactions was previously shown and, therefore, we wanted to investigate the resulting effect of the surface modification with NHCs on the activity of the catalyst.<sup>13</sup>

Our method of choice for the synthesis of different NHC-modified Ru/K-Al<sub>2</sub>O<sub>3</sub>-catalysts was the generation of the free NHC by deprotonation of the corresponding imidazolium tetrafluoroborate salts with potassium *tert*-butoxide in solution and, after filtration, the impregnation of the free NHCs (dicyclohexylimidazolylidene = ICy (1) and dimesitylimidazolylidene = IMes (2)) on Ru/K-Al<sub>2</sub>O<sub>3</sub> (Ru: 4 wt%, K: 4 wt%) (Scheme 1). The amount of 1 and 2 was initially fixed to ~1/2 (in a molar ratio) that of surface Ru to ensure possible adsorption of the substrate onto the heterogeneous catalyst (preparation details are presented in Supporting Information). By our method, we could avoid impurities on the catalyst resulting from the generation of the free NHC *in situ*, which would dramatically complicate structural analysis. Additionally, this method is applicable to a variety of NHCs because isolation of the free NHC is not required, which significantly reduces the possibility of NHC-dimerization.

With this method in hand, we were able to prepare the corresponding NHC-modified Ru/K-Al<sub>2</sub>O<sub>3</sub> catalysts (denoted as 1@Ru/K-Al<sub>2</sub>O<sub>3</sub> and 2@Ru/K-Al<sub>2</sub>O<sub>3</sub>) that could be analyzed by various surface characterization techniques to elucidate the nature of the NHC-catalyst interaction. By monitoring the signal of the free carbene carbon atom of the NHCs with <sup>13</sup>C solid-state NMR, we wanted to investigate whether both NHCs are bound to Ru-NPs or only adsorbed on the support. Unfortunately, we could not observe the signals attributed to the carbene carbon atom of the NHCs, which is, however, consistent with the literature due to significant peak broadening effects close to the surface.<sup>8,14</sup> Inspired by the seminal work of Chaudret on NHC-

Received: April 13, 2016

Published: August 8, 2016

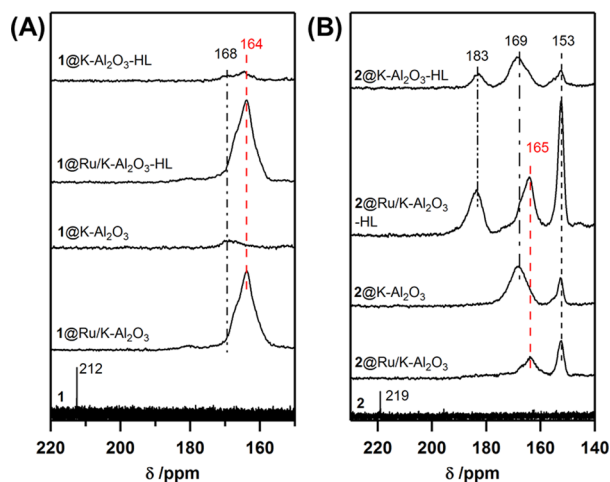


**Figure 1.** (A)  $^{13}\text{C}$  CP-MAS NMR-spectra of  $1@Ru/K\text{-Al}_2\text{O}_3$ ,  $1@K\text{-Al}_2\text{O}_3$ ,  $1@Ru/K\text{-Al}_2\text{O}_3\text{-HL}$ , and  $1@K\text{-Al}_2\text{O}_3\text{-HL}$  (10 kHz) and  $^{13}\text{C}$  NMR spectrum of **1** (in  $\text{C}_6\text{D}_6$ ). (B)  $^{13}\text{C}$  CP-MAS NMR-spectra of  $2@Ru/K\text{-Al}_2\text{O}_3$ ,  $2@K\text{-Al}_2\text{O}_3$ ,  $2@Ru/K\text{-Al}_2\text{O}_3\text{-HL}$ , and  $2@K\text{-Al}_2\text{O}_3\text{-HL}$  (10 kHz), and  $^{13}\text{C}$  NMR spectrum of **2** (in  $\text{C}_6\text{D}_6$ ).

stabilized NPs,<sup>8a</sup> we decided to employ NHCs whose carbene carbon atoms were  $^{13}\text{C}$ -labeled, and due to this modification, we were finally able to observe distinct peaks at 164 ppm for  $1@Ru/K\text{-Al}_2\text{O}_3$  and at 165 ppm  $2@Ru/K\text{-Al}_2\text{O}_3$  (Figure 1) that were upfield shifted from those of the corresponding free NHCs (212 ppm for **1** and 219 ppm for **2**) and are in the range of NHCs bound to transition metals.<sup>4,15</sup> To rule out if the NHC is only adsorbed on the support, we applied our method to pure  $\text{K-Al}_2\text{O}_3$  without Ru-NPs (denoted as  $1@K\text{-Al}_2\text{O}_3$  and  $2@K\text{-Al}_2\text{O}_3$ ). As for  $1@K\text{-Al}_2\text{O}_3$ , a peak was observed at a slightly different position (168 ppm), and its intensity was very low, suggesting that only traces of **1** are adsorbed on the support. As for  $2@K\text{-Al}_2\text{O}_3$ , we observed a peak at 169 ppm, whose chemical shift was obviously different from that of  $2@Ru/K\text{-Al}_2\text{O}_3$ . These results indicate that the carbene carbon atoms of **1** and **2** were mainly attached to Ru-NPs.<sup>16</sup> A peak at 153 ppm was observed in both  $2@Ru/K\text{-Al}_2\text{O}_3$  and  $2@K\text{-Al}_2\text{O}_3$ . This is, probably, due to interactions of the electron-rich  $\pi$ -system of the aromatic N-substituents with the Lewis-acidic sites of the support.<sup>17</sup> (NMR spectra of whole region are shown in Figure S1).

To further prove the presence of the NHC on the surface of the catalyst, we performed X-ray photoelectron spectroscopy (XPS) analysis with high sensitivity for nitrogen. We were able to exclusively observe N 1s signals for  $1@Ru/K\text{-Al}_2\text{O}_3$  and  $2@Ru/K\text{-Al}_2\text{O}_3$ : the peaks were observed at 397–403 eV for the N 1s region (Figures 2A, S2), although peak deconvolution was not possible due to low signal intensities. No N 1s signal was observed for  $Ru/K\text{-Al}_2\text{O}_3$  in the absence of NHCs (Figure 2A). FT-IR of  $1@Ru/K\text{-Al}_2\text{O}_3$  exhibited peaks at 2859 and 2938  $\text{cm}^{-1}$  (C–H stretching of **1**), which were not observed in  $Ru/K\text{-Al}_2\text{O}_3$  (for FT-IR spectra see Figure S3). Furthermore, the weight loss determined by thermogravimetric analysis (TGA) analysis (for TGA data see Figure S4, Table S1) for  $1@Ru/K\text{-Al}_2\text{O}_3$  is attributed to **1** (0.78 wt%). All of these results support the NMR observations that **1** is present on the catalyst surface.

To analyze the effect of our modification method on the Ru-NPs, we performed transmission electron microscopy (TEM), Ru 3p XPS, and Ru K-edge extended X-ray absorption fine structure (EXAFS). TEM analyses of  $1@Ru/K\text{-Al}_2\text{O}_3$  and  $2@Ru/K\text{-Al}_2\text{O}_3$  clearly showed no change in NP size after

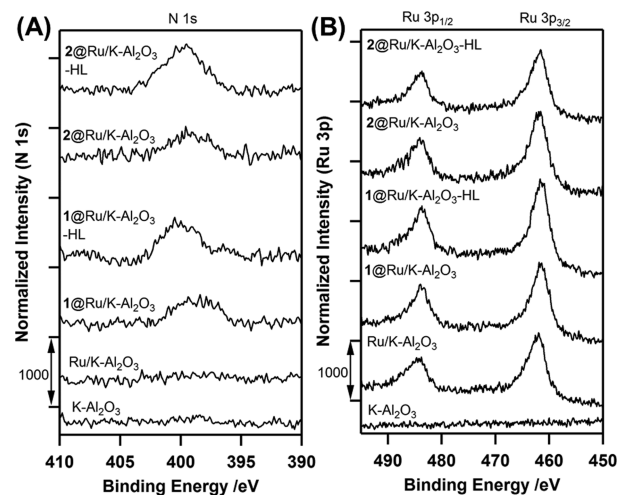


**Figure 2.** Normalized (A) N 1s and (B) Ru 3p XPS spectra of  $1@Ru/K\text{-Al}_2\text{O}_3$ ,  $2@Ru/K\text{-Al}_2\text{O}_3$ ,  $1@Ru/K\text{-Al}_2\text{O}_3\text{-HL}$ ,  $2@Ru/K\text{-Al}_2\text{O}_3\text{-HL}$ ,  $Ru/K\text{-Al}_2\text{O}_3$ , and  $K\text{-Al}_2\text{O}_3$ .

attachment of each NHC (Figure S5). The average particle sizes of  $1@Ru/K\text{-Al}_2\text{O}_3$  and  $2@Ru/K\text{-Al}_2\text{O}_3$  were both  $1.5 \pm 0.7$  nm, which were comparable to that of unmodified  $Ru/K\text{-Al}_2\text{O}_3$  ( $1.5 \pm 0.7$  nm) (Figure S5). The Ru 3p XPS signals were observed at 462 eV ( $Ru\ 3p_{3/2}$ ) and 484 eV ( $Ru\ 3p_{1/2}$ ), which are similar for  $1@Ru/K\text{-Al}_2\text{O}_3$ ,  $2@Ru/K\text{-Al}_2\text{O}_3$ , and  $Ru/K\text{-Al}_2\text{O}_3$  (Figures 2B, S2), suggesting that the difference in oxidation state of Ru before and after the attachment of NHCs was negligible. Furthermore, the peak intensities were almost identical, supporting the fact that the dispersion degree of Ru on the  $\text{K-Al}_2\text{O}_3$  surface was almost the same before and after the attachment of the NHCs which supports the results generated by TEM. The coordination numbers (CNs) of Ru–Ru on  $1@Ru/K\text{-Al}_2\text{O}_3$  and  $2@Ru/K\text{-Al}_2\text{O}_3$  characterized by Ru K-edge EXAFS (Figures S6, S7, Table S2) were  $3.9 \pm 0.8$  and  $4.2 \pm 0.7$ , respectively (bond length ( $R$ ) for  $1@Ru/K\text{-Al}_2\text{O}_3$ :  $0.266 \pm 0.001$  nm,  $R$  for  $2@Ru/K\text{-Al}_2\text{O}_3$ :  $0.266 \pm 0.001$  nm) which were comparable to that of  $Ru/K\text{-Al}_2\text{O}_3$  (CN =  $3.9 \pm 1.0$ ,  $R = 0.266 \pm 0.001$  nm), additionally supporting the nature of Ru-NPs to be unchanged before and after the NHC-attachment. The results of these analytical methods, therefore, clearly demonstrate that the Ru-NPs, which are directly attached on the oxide surface, can be modified by NHCs without rearrangement or decomposition of the Ru-NP itself.

Excited about the observation that the NHC binds as a carbene to Ru, we were intrigued to characterize modified  $Ru/K\text{-Al}_2\text{O}_3$  catalysts with a higher amount of attached NHC. We characterized NHC-attached  $Ru/K\text{-Al}_2\text{O}_3$  catalysts (denoted as  $1@Ru/K\text{-Al}_2\text{O}_3\text{-HL}$  and  $2@Ru/K\text{-Al}_2\text{O}_3\text{-HL}$ , respectively (HL represents high loading). The added amount of **1** and **2** was now fixed to be  $\sim 3$  equiv to that of surface Ru (in a molar ratio). Therefore, we expected the surface of Ru-NPs to be fully covered with NHCs.

The  $^{13}\text{C}$  solid-state NMR of  $^{13}\text{C}$ -labeled  $1@Ru/K\text{-Al}_2\text{O}_3\text{-HL}$  exhibited strong peaks at 164 ppm, which are at the same position as  $1@Ru/K\text{-Al}_2\text{O}_3$  but different from  $1@K\text{-Al}_2\text{O}_3\text{-HL}$  (the sample prepared by the impregnation of **1**, the amount of which was the same as  $1@Ru/K\text{-Al}_2\text{O}_3\text{-HL}$ , on  $\text{K-Al}_2\text{O}_3$  without Ru-NP: 168 ppm) (Figure 1A), indicating that **1** was mainly attached to Ru-NPs.<sup>16</sup> From the N 1s XPS spectrum of  $1@Ru/K\text{-Al}_2\text{O}_3\text{-HL}$ , the peak intensity was higher than that of  $1@Ru/K\text{-Al}_2\text{O}_3$ , suggesting that the amount of **1** attached on  $1@Ru/K\text{-Al}_2\text{O}_3\text{-HL}$

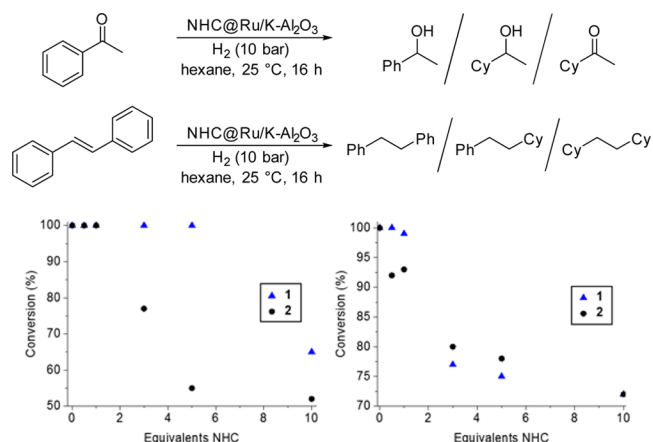
was higher than that on  $1@Ru/K-Al_2O_3$  (Figure 2A). The intensity of C–H vibration region peaks of  $1@Ru/K-Al_2O_3$ -HL in the FT-IR spectrum was higher, and the weight loss (2.0 wt%) by TGA analysis of  $1@Ru/K-Al_2O_3$ -HL was larger than that of  $1@Ru/K-Al_2O_3$  as well, supporting that a higher amount of **1** is present on the surface (Figures S3, S4 and Table S1).

The  $^{13}C$  solid-state NMR of  $^{13}C$ -labeled  $2@Ru/K-Al_2O_3$ -HL was significantly different from the spectra of  $2@Ru/K-Al_2O_3$  (Figure 1B). A new peak at 183 ppm was observed together with a peak at 165 ppm, attributed to the carbene carbon directly attached to the Ru-NPs,<sup>16</sup> and a peak at 153 ppm attributed to the adsorption of the NHC on the support via the electron-rich  $\pi$ -systems of the aromatic N-substituents. The previously not observed peak (183 ppm) was also observed on  $2@K-Al_2O_3$ -HL without Ru-NPs; therefore, it is suggested that this peak was also derived from **2** being adsorbed onto the support. In the N 1s XPS spectrum of  $2@Ru/K-Al_2O_3$ -HL, the peak intensity was larger than that of  $2@Ru/K-Al_2O_3$ , suggesting that the amount of **2** attached on  $2@Ru/K-Al_2O_3$ -HL was also larger than that of  $2@Ru/K-Al_2O_3$ , which is further supported by the FT-IR and TGA analyses (Figures S3, S4).

The average particle sizes of  $1@Ru/K-Al_2O_3$ -HL and  $2@Ru/K-Al_2O_3$ -HL from TEM analyses (Figure S5) were estimated to be  $1.6 \pm 0.8$  and  $1.5 \pm 0.6$  nm, respectively, which were comparable to those of  $1@Ru/K-Al_2O_3$  and  $2@Ru/K-Al_2O_3$ . The Ru 3p XPS signals of  $1@Ru/K-Al_2O_3$ -HL and  $2@Ru/K-Al_2O_3$ -HL were observed at 462 eV (Ru 3p<sub>3/2</sub>) and 484 eV (Ru 3p<sub>1/2</sub>), the positions of which were similar to  $1@Ru/K-Al_2O_3$  and  $2@Ru/K-Al_2O_3$  (Figure 2B), and the peak intensities were also almost identical. The CNs of Ru–Ru on  $1@Ru/K-Al_2O_3$ -HL and  $2@Ru/K-Al_2O_3$ -HL characterized by Ru K-edge EXAFS (Figures S6, S7, Table S2) were  $4.2 \pm 0.6$  and  $3.9 \pm 0.9$ , respectively, ( $R$  for  $1@Ru/K-Al_2O_3$ -HL:  $0.267 \pm 0.001$  nm,  $R$  for  $2@Ru/K-Al_2O_3$ -HL:  $0.266 \pm 0.001$  nm), which were comparable to that of  $1@Ru/K-Al_2O_3$  and  $2@Ru/K-Al_2O_3$  as well. These results indicate that the nature of Ru-NPs is not affected even at an increased amount of attached NHCs.

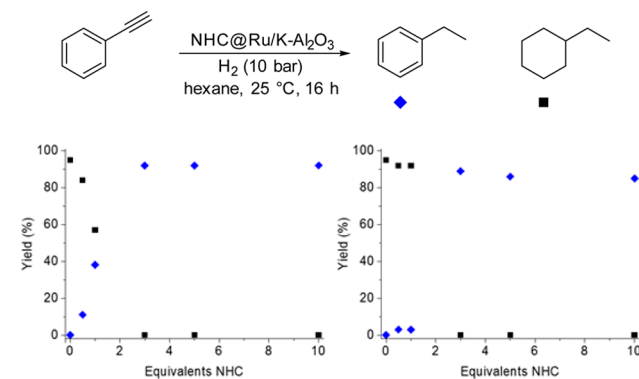
With the detailed characterization of the catalyst with different amounts of NHC and the nature of the NHC-binding in hand, we started to investigate the effect of the NHCs (**1** and **2**) on the reactivity and selectivity of benchmark reactions. We chose acetophenone, *trans*-stilbene, octene, and isophorone as our model substrates, as they contain classical functional groups that can be hydrogenated by heterogeneous Ru-catalysts (Scheme 2, Tables S3, S4).<sup>18</sup> Starting from unmodified Ru/K-Al<sub>2</sub>O<sub>3</sub> to 1 equiv of NHC per surface Ru (in a molar ratio), we could not observe any decrease in activity for the hydrogenation of *trans*-stilbene. However, by increasing the amount to 3 equiv of NHC for  $2@Ru/K-Al_2O_3$ , a decrease in conversion of 25% could be detected, whereas a significant decrease in conversion for  $1@Ru/K-Al_2O_3$  could not be observed until 10 equiv of **1** to surface Ru was employed. With 10 equiv of NHC, a decrease in conversion for *trans*-stilbene of 40% for **1** and of 50% for **2**, respectively, was observed, suggesting that not only the amount but also the nature of the NHC affects the reactivity of the catalyst (Scheme 2). In contrast to *trans*-stilbene, an effect at lower amounts of NHC could be observed for the hydrogenation of acetophenone. Already at 0.5 equiv of NHC to surface Ru (in a molar ratio), a decrease in conversion up to 5% for **1** and 10% for **2** was obtained. Increasing the amount of NHC continuously leads to a drop of conversion of acetophenone of 30% for **1** and **2**, respectively. In accordance to the hydrogenation of *trans*-stilbene, the nature of the NHC is crucial for the reduction of

### Scheme 2. Effect of NHC-Loading on the Hydrogenation of Acetophenone and *trans*-Stilbene<sup>a</sup>



<sup>a</sup>Conversion determined by GC-FID analysis. Hydrogenation of (left) *trans*-stilbene and (right) acetophenone.

### Scheme 3. Effect of NHC-Loading on the Chemoselectivity in the Hydrogenation of Phenyl Acetylene<sup>a</sup>



<sup>a</sup>Conversion determined by GC-FID analysis: (left) **1** and (right) **2**.

activity, as the catalyst activity is reduced more significantly by **2** than by **1**. The general trend that the activity of the catalyst is reduced by an increasing amount of NHC can be explained by the fact that more active sites of the catalyst are blocked by the NHC; therefore, less active sites are accessible for the substrates leading to a diminished conversion. The higher steric bulk of the N-substituents of **2** in comparison to **1** displays a possible reason for the more significant drop in conversion, as more active sites are shielded by **2** than by **1**.<sup>15</sup>

Encouraged by these results, we decided to design an NHC-tunable system for the chemoselective hydrogenation of phenyl acetylene that contains two chemically different functional groups (Scheme 3, Tables S5, S6).<sup>19</sup> Hydrogenation of the benzene moiety is more difficult than hydrogenation of the alkyne unit, which should give rise to chemoselectivity by tuning the catalyst activity by the amount of attached NHC. At amounts of up to 0.5 equiv of NHC to surface Ru (in a molar ratio), no dramatic change in chemoselectivity could be observed for **1** and **2**. Increasing the amount to 1 equiv of NHC provided almost an equimolar mixture for **1** as ligand, whereas the complete hydrogenation of the triple bond and the benzene moiety was obtained with **2** as ligand. Further increasing of the amount of NHC led to a dramatic increase in chemoselectivity, as the hydrogenation of the triple bond occurred exclusively for both

NHCs. Due to the higher amount of NHC on the support, there is less free space on the catalyst for the adsorption of the substrate, leading to the exclusive adsorption of the smaller alkyne moiety. The more drastic change in chemoselectivity for **2** compared to **1** can be attributed to the higher steric demand of the N-substituents of **2**.<sup>15</sup>

Because of the fact that leaching is a common problem in heterogeneous catalysis, we decided to analyze the reaction solution by total reflection X-ray fluorescence spectroscopy (TXRF) and mass spectrometry at the end of the reaction to get an insight into possible leaching processes. No Ru-NHC complexes could be detected by mass spectrometry (Tables S10, S11). By TXRF, a ruthenium amount of <0.5 ppm Ru in solution was determined (Table S12).<sup>20</sup> Furthermore, TEM images of the catalysts after the hydrogenation reaction exhibited similar morphology as observed before the reaction, although the particle size became slightly larger (Figure S8). These observations and the fact that leaching is unlikely to occur under reductive conditions<sup>21</sup> support that the hydrogenation is likely to occur in a heterogeneous fashion.

Due to an extensive structural analysis of a NHC-modified supported heterogeneous catalyst, the effect of the NHC modification on the structure of the catalyst could be elucidated, and it could be proven that the NHC binds via the carbene carbon atom to the Ru-NPs. Furthermore, the tunability of Ru/K-Al<sub>2</sub>O<sub>3</sub> by NHCs could be demonstrated by a perfectly chemoselective hydrogenation. This is, truly, a vantage point for the exploration of NHCs as ligands for supported heterogeneous catalysts.

## ■ ASSOCIATED CONTENT

### ● Supporting Information

The Supporting Information is available free of charge on the ACS Publications website at DOI: 10.1021/jacs.6b03821.

Experimental details and data (PDF)

## ■ AUTHOR INFORMATION

### Corresponding Authors

\*smuratsugu@chem.nagoya-u.ac.jp

\*glorius@uni-muenster.de

### Notes

The authors declare no competing financial interest.

## ■ ACKNOWLEDGMENTS

Generous financial support by the Fonds der Chemischen Industrie (J.B.E.), the Deutsche Forschungsgemeinschaft (Leibniz Award and SFB 858), JSPS Funding Program for Next Generation World-Leading Researchers (GR090), MEXT/JSPS KAKENHI grants no. 26620043, and JSPS Core-to-Core Program “Elements Function for Transformative Catalysis and Materials” are gratefully acknowledged. XAFS measurements were performed with the approval of PF-PAC (2013G197 and 2014G060). XPS measurements were conducted at Nagoya University Nanofabrication Platform, supported by “Nanotechnology Platform Program” of MEXT, Japan. We thank A. Kodaira for XPS and TGA measurements. TEM measurements were conducted at High Voltage Electron Microscope Laboratory, Institute of Materials and Systems for Sustainability, Nagoya University, supported by “Advanced Characterization Nanotechnology Platform” of MEXT, Japan, and we thank K. Higuchi for TEM measurements. We thank M. Holtkamp for TXRF measurements.

## ■ REFERENCES

- (1) Hopkinson, M. N.; Richter, C.; Schedler, M.; Glorius, F. *Nature* **2014**, *510*, 485.
- (2) (a) Fortman, G. C.; Nolan, S. P. *Chem. Soc. Rev.* **2011**, *40*, 5151. (b) Kantchev, E. A. B.; O'Brien, C. J.; Organ, M. G. *Angew. Chem., Int. Ed.* **2007**, *46*, 2768.
- (3) Vougioukalakis, G. C.; Grubbs, R. H. *Chem. Rev.* **2010**, *110*, 1746.
- (4) Zhukhovitskiy, A. V.; MacLeod, M. J.; Johnson, J. A. *Chem. Rev.* **2015**, *115*, 11503.
- (5) Examples for the modification of Au surfaces: (a) Weidner, T.; Baio, J. E.; Mundstock, A.; Grosse, C.; Karthaus, S.; Bruhn, C.; Siemeling, U. *Aust. J. Chem.* **2011**, *64*, 1177. (b) Zhukhovitskiy, A. V.; Mavros, M. G.; Van Voorhis, T.; Johnson, J. A. *J. Am. Chem. Soc.* **2013**, *135*, 7418. (c) Crudden, C. M.; Horton, J. H.; Ebraldize, I. I.; Zenkina, O. V.; McLean, A. B.; Drevniok, B.; She, Z.; Kraatz, H. B.; Mosey, N. J.; Seki, T.; Keske, E. C.; Leake, J. D.; Rousina-Webb, A.; Wu, G. *Nat. Chem.* **2014**, *6*, 409.
- (6) Hurst, E. C.; Wilson, K.; Fairlamb, I. J. S.; Chechik, V. *New J. Chem.* **2009**, *33*, 1837.
- (7) Vignolle, J.; Tilley, T. D. *Chem. Commun.* **2009**, 7230.
- (8) (a) Lara, P.; Rivada-Wheelaghan, O.; Conejero, S.; Poteau, R.; Philippot, K.; Chaudret, B. *Angew. Chem., Int. Ed.* **2011**, *50*, 12080. (b) Gonzalez-Galvez, D.; Lara, P.; Rivada-Wheelaghan, O.; Conejero, S.; Chaudret, B.; Philippot, K.; van Leeuwen, P. W. N. M. *Catal. Sci. Technol.* **2013**, *3*, 99. (c) Lara, P.; Suarez, A.; Colliere, V.; Philippot, K.; Chaudret, B. *ChemCatChem* **2014**, *6*, 87. (d) Baquero, E. A.; Tricard, S.; Flores, J. C.; de Jesus, E.; Chaudret, B. *Angew. Chem., Int. Ed.* **2014**, *53*, 13220. (e) Martínez-Prieto, L. M.; Ferry, A.; Rakers, L.; Richter, C.; Lecante, P.; Philippot, K.; Chaudret, B.; Glorius, F. *Chem. Commun.* **2016**, *52*, 4768.
- (9) (a) Richter, C.; Schaepe, K.; Glorius, F.; Ravoo, B. J. *Chem. Commun.* **2014**, *50*, 3204. (b) Ferry, A.; Schaepe, K.; Tegeder, P.; Richter, C.; Chepiga, K. M.; Ravoo, B. J.; Glorius, F. *ACS Catal.* **2015**, *5*, 5414. (c) Rühling, A.; Schaepe, K.; Rakers, L.; Vonhören, B.; Tegeder, P.; Ravoo, B. J.; Glorius, F. *Angew. Chem., Int. Ed.* **2016**, *55*, 5856.
- (10) MacLeod, M. J.; Johnson, J. A. *J. Am. Chem. Soc.* **2015**, *137*, 7974.
- (11) (a) Ranganath, K. V. S.; Kloesges, J.; Schäfer, A. H.; Glorius, F. *Angew. Chem., Int. Ed.* **2010**, *49*, 7786. (b) Ranganath, K. V. S.; Onitsuka, S.; Kumar, A. K.; Inanaga, J. *Catal. Sci. Technol.* **2013**, *3*, 2161.
- (12) Schüth, F. *Chem. Unserer Zeit* **2006**, *40*, 92.
- (13) Muratsugu, S.; Kityakarn, S.; Wang, F.; Ishiguro, N.; Kamachi, T.; Yoshizawa, K.; Sekizawa, O.; Uruga, T.; Tada, M. *Phys. Chem. Chem. Phys.* **2015**, *17*, 24791.
- (14) Pan, C.; Pelzer, K.; Philippot, K.; Chaudret, B.; Dassenoy, F.; Lecante, P.; Casanove, M.-J. *J. Am. Chem. Soc.* **2001**, *123*, 7584.
- (15) Dröge, T.; Glorius, F. *Angew. Chem., Int. Ed.* **2010**, *49*, 6940.
- (16) To further support the binding of the NHC to Ru-NPs, we performed reactions with **1**@Ru/K-Al<sub>2</sub>O<sub>3</sub> (2 wt% Ru) and observed similar behaviour as for **1**@Ru/K-Al<sub>2</sub>O<sub>3</sub> (4 wt% Ru). For details see Tables S7 and S8.
- (17) For examples of adsorption of aromatic compounds on metal-oxide supports: (a) Popov, A.; Kondratieva, E.; Goupil, J. M.; Mariey, L.; Bazin, P.; Gilson, J.-P.; Travert, A.; Maugé, F. *J. Phys. Chem. C* **2010**, *114*, 15661. (b) Scire, S.; Crisafulli, C.; Maggiore, R.; Minico, S.; Galvagno, S. *Appl. Surf. Sci.* **1996**, *93*, 309. (c) Shabalin, I. I.; Kiva, E. A.; Churkin, Y. V.; Rusanova, L. A.; Mazitov, M. F. *Kinet. Catal.* **1974**, *15*, 1360. (d) Taylor, D. R.; Ludlum, K. H. *J. Phys. Chem.* **1972**, *76*, 2882.
- (18) No effect on the conversion of isophorone and octene could be observed.
- (19) In the presence of already small amounts PPh<sub>3</sub> instead of an NHC as ligand, hydrogenation of the aromatic system was completely inhibited. For experimental details see Table S9.
- (20) Holtkamp, M.; Wehe, C. A.; Blaske, F.; Holtschulte, C.; Sperling, M.; Karst, U. *J. Anal. At. Spectrom.* **2012**, *27*, 1799.
- (21) Under reductive conditions, nucleation of reduced metallic species can occur, as minimization of free surface energy is preferred. Widegren, J. A.; Finke, R. G. *J. Mol. Catal. A: Chem.* **2003**, *198*, 317.